Advanced Powder Technology xxx (2016) xxx–xxx

Contents lists available at ScienceDirect

Advanced Powder Technology

journal homepage: www.elsevier.com/locate/apt

Original Research Paper

Synthesis of spinel cobalt oxide nanoparticles using a modified polymeric precursor method

Rodolfo Foster Klein Gunnewiek *, Camilla Floriano Mendes, Ruth Herta Goldschmidt Aliaga Kiminami

Federal University of São Carlos, Department of Materials Engineering, Rod. Washington Luiz, km 235, São Carlos 13565-905, SP, Brazil

ARTICLE INFO

Article history:
Received 23 April 2015
Received in revised form 13 March 2016
Accepted 15 March 2016
Available online xxxx

Keywords:
Spinel cobalt oxide nanoparticles
Ammonium polyacrylate
Modified polymeric precursor method
Complexation

ABSTRACT

Metal oxide nanoparticles have been raising increasing interest. In this work, spinel cobalt oxide (Co_3O_4) nanoparticles of around 29 nm were synthesized using a modified polymeric precursor method. This method is based on the complexation of polyacrylate and cobalt ions in aqueous media by a chelation reaction, resulting in the synthesis of crystalline nanoparticles, confirmed by X-ray diffraction (XRD) and high resolution transmission electron microscopy (HRTEM). Some advantages of this technique are the fast, simple and efficient synthesis of nanoparticles after only 2 h of thermal decomposition at 480 °C and elimination of the aging step, which is an essential step in polymeric precursor-based methods such as sol–gel.

1. Introduction

Spinel cobalt oxide (Co_3O_4) is a material of scientific and technological interest because of its various properties, as well as the fact that it is a magnetic p-type semiconductor with two bandgaps of 2.0 eV and 1.46 eV [1], which interacts in the visible electromagnetic spectrum (absorption and emission) [2,3]. These characteristics make Co_3O_4 suitable for several applications, such as magnetic storage devices [2], electrochemical catalysis and photocatalysis [3–5], improvement of electrode capacity and cycling stability in lithium-ion batteries [2,6,7], electrochemical sensors [4,6], precursors for solid-state synthesis [8], supercapacitors [9,10] and nanofluid coolants [11].

Cobalt presents two main oxidation states: +II and +III. These two valences enable cobalt to form the following oxides: CoO, Co_2O_3 (which exists in the hydrated form), and the more common spinel-type Co_3O_4 (composed of cobalt in +II and +III valences, $CoO{\cdot}Co_2O_3$) [12]. However, because of the polyvalent states of cobalt ion, control of the atmosphere is essential to produce the desired cobalt oxide, while the most suitable synthesis technique must be chosen and conditions controlled to obtain nanoparticles.

In view of the above, researchers have attempted to synthesize cobalt oxide nanoparticles by different methods, such as hydrothermal [1,2], soft chemical method [3,5,11], direct thermal decomposition [6,11], polymer-based synthesis [7,8,13], plasma spray pyrolysis [9], solvothermal synthesis [14], microwave assisted synthesis [10,15], etc. Nonetheless, these techniques have disadvantages, such as long synthesis time, sometimes more than 20 h, and require the use of complex equipment or unusual reactants.

The polymeric precursor method has undergone modifications to make it faster. The complexation of polyacrylate and metal ions in water, followed by thermal decomposition, leads to the synthesis of several oxides with very fine primary particles, such as zirconia, alumina, yttrium, lead and barium titanates [16], and cerium [17]. Recently, Gunnewiek et al. [18] performed rapid synthesis of very fine chromium oxide nanoparticles. Although this technique is very useful and fast, few studies have focused on the use of an aqueous complexation of polyacrylate to synthesize metal oxide nanoparticles. This technique uses simple equipment, aqueous solutions and very common reactants such as ammonium polyacrylate, which is widely employed as a dispersant in ceramic suspensions.

In this study, a rapid, efficient and simple synthesis technique was used based on a modified polymeric precursor method. Pure spinel-type cobalt oxide nanoparticles were easily fast-synthesized in only 6–7 h. The technique consists in a water-based complexation reaction between polyacrylic anions and cobalt cations, which takes only ten minutes, followed by freeze drying and rapid thermal decomposition at a relatively low temperature, resulting in highly crystallized nanoparticles. In addition, the optimal condition of thermal decomposition temperature was determined and the nanoparticles were characterized.

* Corresponding author. Tel.: +55 3536974600.
E-mail address: rodolfo.foster@unifal-mg.edu.br (R.F.K. Gunnewiek).

http://dx.doi.org/10.1016/j.apt.2016.03.013
0921-8831/

2. Experimental procedure

2.1. Polymeric complexation

$Co(NO_3)_2{\cdot}6H_2O$ (Sigma–Aldrich, >98%) 0.5 M was prepared and stir-mixed into a solution of ammonium polyacrylate (molecular weight ~4500, Lamberti-Reotan LA) (15 wt.%, pH 8.0). The reaction was conducted at room temperature, mixing the cobalt nitrate and PA solutions (1:2-volume) under constant stirring. A purple metal-polymeric flocculated complex was formed (PA-Co) instantaneously. The PA-Co complex was washed and centrifuged three times to remove undesirable soluble ions. Both complex and washing water were very stable and their color did not change. The resinous complex was resuspended and freeze dried (Edwards Micro Modulyo), yielding a very fluffy powder in less than 3 h.

2.2. Thermal decomposition and characterization

The optimal temperature for thermal decomposition was determined by thermogravimetric analysis (TGA) and differential thermal calorimetry (DSC) (Netzsch STA 449 C), heated at 5 °C/min, from room temperature to 750 °C. The sample was then thermally decomposed at the same heating rate, with a soak of 120 min at the optimal temperature.

The material was subjected to X-ray diffractometry (Siemens D5005) to characterize its crystallinity, index the phase sand identify the lattice parameters, using Kα radiation of copper ($\lambda = 1.54$ Å). The 2θ range varied from 20° to 80°, and planes distances and cell parameters (a and volume) were calculated. The planar distances were calculated using Bragg's equation:

$$n\lambda = 2d_{hkl} * \sin\theta \quad (1)$$

The lattice parameter a and cell volume, V, were calculated as [19]:

$$1/d^2 = (h^2 + k^2 + l^2)/a^2 \quad (2)$$

$$V = a^3 \quad (3)$$

The average crystallite size, t, was estimated using Scherrer's equation (Eq. (4)), where B is the peak broadening at full width half maximum (FWHM), and θ is the diffraction angle.

$$t = 0.9\lambda/B * \cos\theta \quad (4)$$

The as-synthesized powder was deagglomerated in a mortar, resulting in a very fine dark powder. For the surface area (S_{BET}) analysis, the surface of powder was cleaned by treating it thermally at 180 °C under vacuum for two hours. The S_{BET} was determined using the cold N_2 adsorption/desorption technique (Micromeritics ASAP 2020), calculated by the Brunauer–Emmet–Teller (BET) equation. The average spherical particle size (d_{BET}) was estimated from the Eq. (5), where ρ_{th} is the theoretical density for Co_3O_4 (6.055 g/cm^3).

$$d_{BET} = 6/(S_{BET} * \rho_{th}) \quad (5)$$

Micrographs of the powder morphology were recorded with a scanning electron microscope (SEM, Philips XL30 FEG). The powder was dispersed ultrasonically in acetone and dripped onto the aluminum sample holder. After it dried, a very thin gold layer was sputtered onto the sample. Micrographs were also recorded by transmission electron microscopy (TEM), select area electron diffraction (SAED), and high resolution transmission electron microscopy (HRTEM) (FEI Tecnai G2F20). The primary particle size was measured using an image analyzer program. Around 65 particles were counted in four TEM images of different regions of the same sample.

3. Results and discussion

Fig. 1(a) depicts the thermogravimetric analysis (line) and the first derivative (d(TGA)/dt) curve of the dry fluffy complex, showing weight loss as a function of temperature, while Fig. 1(b) depicts the DSC curve. Note the presence of four peaks on the derivative curve (Fig. 1(a)) corresponding to the following temperatures: a maximum peak at around 50 °C, which corresponds to water adsorption, a peak with minimum at 221 °C, followed by another at 257 °C, and lastly a peak between 380 and 459 °C.

The mass increase below 50 °C is associated with water adsorption (a well defined peak on the DSC curve). This water loss occurs at about 100 °C. An exothermic peak occurs at around 180 °C, followed by another at approximately 225 °C, with a mass loss of about 30%. We believe that the peaks at 221 and 257 °C correspond to the initial decomposition and formation of intermediary phases, and that the final range (from 380 to 459 °C) corresponds to the formation of cobalt oxide. An analysis of the TGA curve indicates that mass loss above 460 °C is very low. There are corresponding inflexions on the dTGA curve, indicating the onset of thermal decomposition reactions. The last reaction step occurs at 370 °C (an inflexion on the dTGA curve and an endothermic peak on the DSC curve), ending at 460 °C. The latter step is believed to be associated with the formation of cobalt oxide, and the decomposition temperature was set at 480 °C, heating rate of 5 °C/min, and a soak

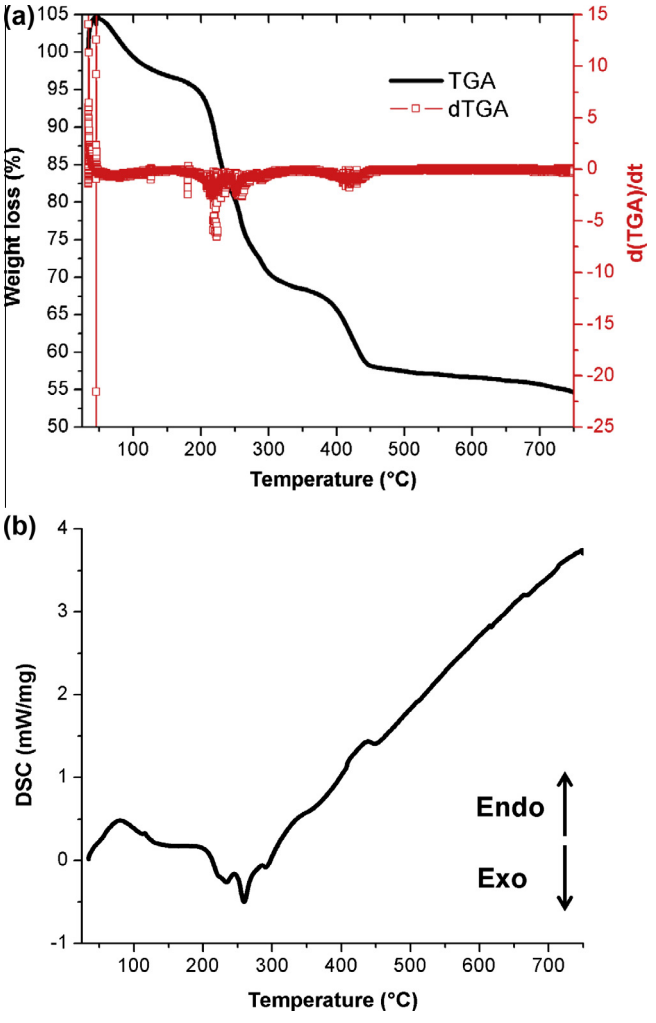

Fig. 1. (a) Thermogravimetric analysis and first derivative curve, and (b) DSC curve of the PA-Co complex.

Please cite this article in press as: R.F.K. Gunnewiek et al., Synthesis of spinel cobalt oxide nanoparticles using a modified polymeric precursor method, Advanced Powder Technology (2016), http://dx.doi.org/10.1016/j.apt.2016.03.013

time of 120 min. Above 690 °C is possible to see a moderate mass loss of around 1.2%, which we believe to be associated to cobalt oxide evaporation.

The Fig. 2 depicts the diffractograms of powders calcined at three different temperatures (270, 360 and 480 °C), corresponding to important regions of the thermal analysis.

The diffractogram of powder calcined at 270 °C shows very modest peaks, indicating the initial decomposition of polyacrylate/cobalt complex and initial formation of cobalt oxide. As proposed before, this temperature led to formation of intermediate compounds, mostly amorphous or poorly crystalline, since there are no important peaks. Rising the temperature to 360 °C, which correspond to the second important region in TGA curve, the peaks of a crystalline phase are more evident, but still not very defined.

The diffractogram of powder calcined at 480 °C shows very well defined peaks, indicating highly crystalline phase. The spinel cobalt oxide (Co_3O_4) is the stable product at room temperature, when synthesized at higher O_2 partial pressure [8]. However, cobalt oxide II (CoO) can be stable when nanoparticles are produced. The material was analyzed by XRD to confirm which phase was synthesized. When indexed, the peaks coincided with the Co_3O_4 cubic spinel structure (JCPDS card number 74-2120). This phase corresponds to the face-centered cubic structure of the space group Fd-3m. The shape in the diffractogram (Fig. 2) coincides with those presented in earlier reports [6–8].

The planar distance of each diffraction peak, theoretical (d_{th}) and experimental (d_{exp}), was calculated using Eq. (1). The data used to calculate the theoretical interplanar distance of each diffraction peak was found in JCPDS card no. 74-2120. Table 1 lists the calculated parameters. Very minor difference between theoretical and experimental interplanar distances can be noted.

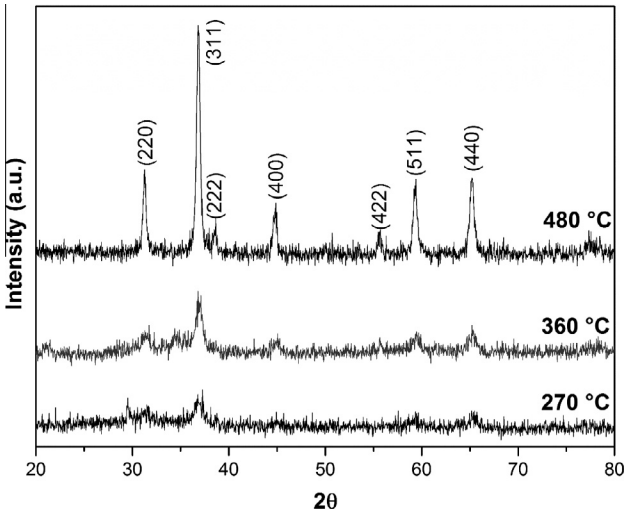

Fig. 2. X-ray diffractogram of the as-synthesized powder at different temperatures: 270, 360 and 480 °C, showing the presence of highly crystalline spinel Co_3O_4 (all the peaks coincide with those of JCPDS card no.74-2120) at 480 °C.

Table 1
Theoretical and experimental values for 2θ and planar distance.

Plane	$2\theta_{th}$	$2\theta_{exp}$	d_{th} (Å)	d_{exp} (Å)
220	31.263	31.264	2.858	2.859
311	36.837	36.842	2.437	2.438
222	38.537	38.580	2.334	2.332
400	44.798	44.784	2.021	2.022
422	55.641	55.671	1.650	1.650
511	59.338	59.324	1.556	1.557
440	65.214	65.201	1.429	1.430

Table 2
Lattice parameter a and cell volume V for each diffraction plane.

Plane	a_{th} (Å)	a_{exp} (Å)	V_{th} (nm^3)	V_{exp} (nm^3)
220	8.0839	8.0853	0.5283	0.5286
311	8.0839	8.0846	0.5283	0.5284
222	8.0842	8.0772	0.5283	0.5270
400	8.0840	8.0880	0.5283	0.5291
422	8.0838	8.0818	0.5283	0.5279
511	8.0842	8.0878	0.5283	0.5290
440	8.0842	8.0876	0.5283	0.5290

The lattice parameter a and cell volume V, both theoretical (a_{th}, V_{th}) (based on JCPDS card no. 74-2121) and experimental (a_{exp}, V_{exp}), were calculated using Eqs. (2) and (3), and the results are described in Table 2. An analysis of the lattice parameter a indicates that the experimental data show very similar values, with an average a_{exp} = 8.0846 Å indicating a regular cubic structure with a deviation of less than 0.004 Å, and a_{th} = 8.0840 Å with a deviation of less than 0.0002 Å. Since the volume is calculated as a function of a, the experimental values follow the same pattern, with average V_{exp} = 0.5284 nm^3, with a very low deviation of less than 0.008 nm^3, while the deviation for the theoretical volume is lower than 0.0003 nm^3 for an average V_{th} = 0.5283 nm^3. This deviation is depicted in Fig. 3, in which the theoretical and experimental cell volumes and lattice parameters are plotted, clearly showing the very minor deviations for a and V.

The broadening of the diffraction peaks (Fig. 2) suggests the presence of small particles. The calculated average crystallite size (Eq. (4)) at the peaks of planes (2 2 0) and (3 1 1) showed very similar values, i.e., 30 nm and 36 nm.

The measured surface area of the synthesized oxide was 7.52 ± 2.62 m^2/g. The average spherical particle size (Co_3O_4 theoretical density of 6.055 g/cm^3) was calculated using Eq. (5). The calculated value of 132 nm did not coincide with that calculated by the Scherrer equation, suggesting the presence of agglomerates.

The SEM micrograph of the powder (Fig. 4) shows a homogeneous soft fluffy agglomerate containing individual equiaxial nanoparticles with a narrow particle size distribution and an average particle size of 35 nm, confirming the value calculated from the broadened peak in the XRD diffractogram. The d_{BET} confirms the presence of powder agglomerates, which are fragile and easy to grind. This soft-agglomerated powder morphology is a common product of polymeric precursor synthesis [21,22].

The presence of agglomerates was confirmed by SEM (Fig. 4), and their nanoparticle structure was substantiated by TEM. Fig. 5 (a) depicts these nanoparticles, while Fig. 5(b) shows their very small size in greater detail. The SAED pattern of these nanoparticles confirms their high crystallinity, and clearly visible equiaxial

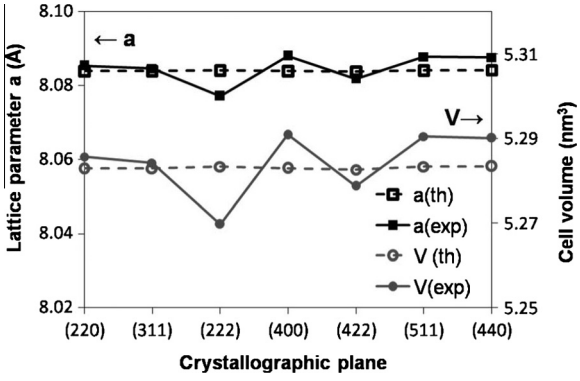

Fig. 3. Lattice parameter a and cell volume as a function of the crystallographic plane.

Please cite this article in press as: R.F.K. Gunnewiek et al., Synthesis of spinel cobalt oxide nanoparticles using a modified polymeric precursor method, Advanced Powder Technology (2016), http://dx.doi.org/10.1016/j.apt.2016.03.013

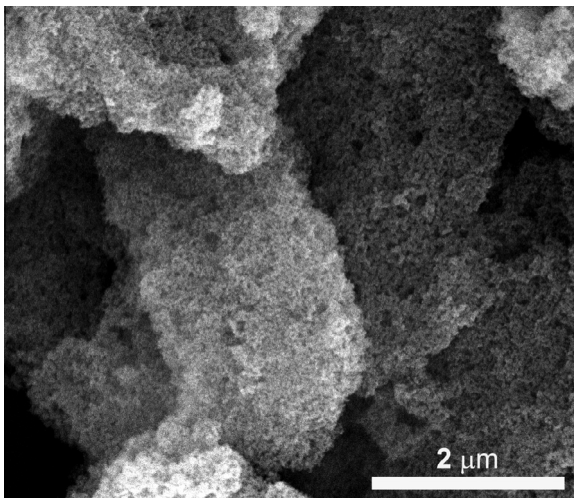

Fig. 4. SEM micrograph of as-synthesized cobalt oxide nanopowder.

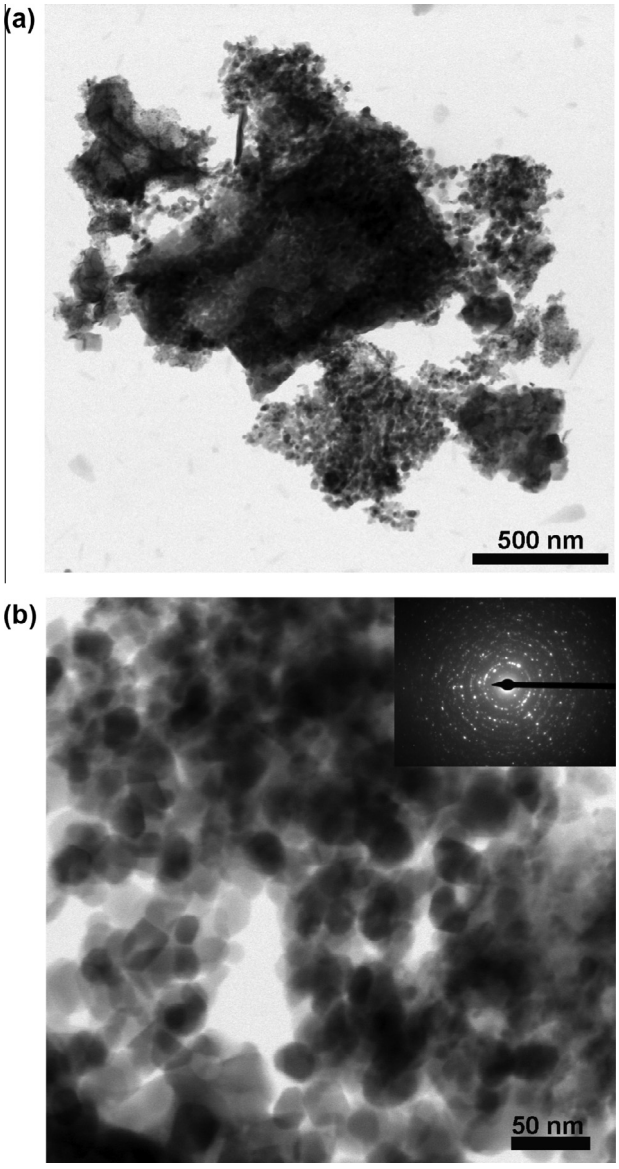

Fig. 5. (a) TEM images showing cobalt oxide nanoparticle agglomerates, and (b) detailed SAED pattern of nanoparticles.

and slightly elongated morphology. In Fig. 5(b), note the average particle size of 29 nm, with a standard deviation of 7 nm.

The HRTEM micrograph in Fig. 6 shows the plane spacing of the nanoparticles and presence of crystals in different directions can be observed. The fringe spacing between two adjacent crystals was also measured. The measured planar distances of 0.218 nm and 0.435 nm can be assigned to the planes (2 2 2) and (1 1 1), respectively, and are very close to the respective theoretical values of 0.233 nm and 0.467 nm.

The EDX pattern in Fig. 6b shows only the presence of cobalt and oxygen elements, confirming the purity of the synthesized cobalt oxide (the peaks corresponding to the elements copper and carbon are attributed to the material of the sample holder). The copper and carbon appearing in EDX are related to the sample holder.

Although the mechanisms involved in this complexation reaction have not yet been clearly established, we believe that the chelation reaction [18,23–26] was responsible for the formation of an insoluble purple complex, which was produced instantaneously upon mixing the cobalt nitrate solution and ammonium polyacrylate. Because the high coordination number of cobalt ions (4 or 6), we expect the complexation occurs when cobalt ions bind to more than one bonding site (carboxylate) of the same molecule (approximately 63 carboxylates in the case of polyacrylate with a molecular weight of 4500), forming a stable structure. Furthermore, linear complexes can coexist, since the polyacrylate chain can bind to only one cobalt ion (or even bind linearly to more than one ion), forming a PA-cobalt network. For the proportion of solutions used (1:2 of cobalt/polyacrylate), and considering the concentration of cobalt solution (0.2 M) and polyacrylate (15%-w), also considering the mean molecular weight of ~4500, there is approximately 20 carboxylate sites per atom of cobalt after mixing the solutions. But the coordination number of cobalt is 4 or 6, which means each atom of cobalt can link to 4 or 6 active carboxylic sites. This reduces the excess to no more than 4–5 times

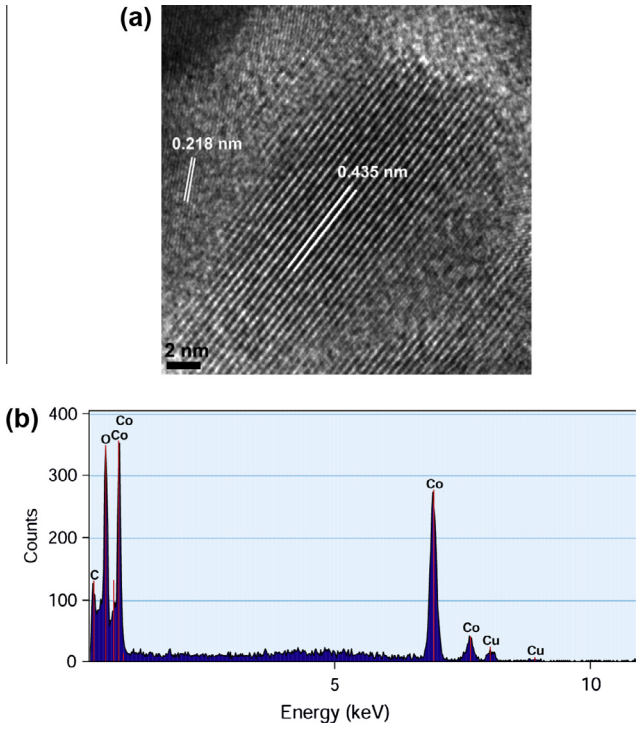

Fig. 6. (a) High resolution TEM image showing d-spacing distances of two crystals, and (b) EDX pattern showing the presence of only cobalt and oxygen.

Please cite this article in press as: R.F.K. Gunnewiek et al., Synthesis of spinel cobalt oxide nanoparticles using a modified polymeric precursor method, Advanced Powder Technology (2016), http://dx.doi.org/10.1016/j.apt.2016.03.013

of carboxylic active sites. The ammonium polyacrylate solution at pH 8.0 is supposed to have all carboxylic sites dissociated. When the transition metal nitrate as cobalt nitrate is added to this solution, it is expected the equilibrium of the reaction is slightly shifted to consume some active sites, turning them undissociated and they are lost. To prevent unlinked cobalt in solution, an excess of polyacrylate was added.

Analogous to the Pechini and sol–gel techniques, the cations bind to the polymer network and present low mobility, but no aging or gelation time was required since the unsoluble complex structure was formed instantaneously. We postulate there is no previous nucleation of any cobalt species since all the cobalt atoms are arrested in the polymeric chain and prevents early undesired nucleation. Moreover, provided they are located at a given atomic distance from each other, powders composed of primary fine particles will be obtained after thermal decomposition of the precursor.

The formation of highly crystalline cobalt oxide undergoes in several steps as organic removal, crystallization and oxidation. The freeze drying allowed to obtain a very fine and fluffy powder and helps the formation of small and separated clusters during the organic removal step. In this step, initially some oxidation around 250–260 °C of the organics led to formation of gaseous species (water and carbon oxides), inducing to some shrinkage in the structure, formation of pores and, the most important, some clusters of amorphous metal oxide. The porous structure will remain until the end of synthesis and will help to produce the soft agglomerates and also maintain the primary crystallites far from each other. Increasing the time and temperature, the continuous organic removal and oxidation of metals occurs. Furthermore, around 270–360 °C the close small clusters will tend to coalesce until critical size, when some small crystalline primary particles appear and grow. Above 460 °C, the particles tend to crystallize well and because the high surface area of small crystallites, the surface atom flux occurs when some particles are in close contact and led to pre-sintering, allowing the porous soft agglomerates in the last step.

The initial oxidation state of the cobalt ion precursor was +II. During the thermal decomposition at low O_2 partial pressure, the ion will retain its oxidation state. Moreover, as mentioned earlier, cobalt II oxide can be retained when the method results in nanoparticles. In this work, the heat treatment was performed in a regular atmosphere, which means an O_2 partial pressure of approximately 0.2 atm. Although nanoparticles were synthesized, the O_2 partial pressure applied here favored the partial oxidation of cobalt from II to III, leaving cobalt in the +III state, leading to the formation of nanoparticles of pure spinel-type cobalt oxide, $CoO{\cdot}Co_2O_3$.

Although this technique is very simple and efficient to synthesize very crystalline cobalt oxide primary nanoparticles of around 29 nm, the process steps must be well controlled. Regarding to water soluble polymer, the size of polymeric chain must be short and present as many as possible reactive groups. The polyacrylate chosen presents relatively short chain (MW of 4800), which contains 63 carboxylate sites. When higher weight molecules are used, there are more reactive sites per molecule but it increases the temperature of calcination [17], which may yield larger crystallite sizes. If there are no sufficient active carboxylate groups to bind to cations, the free cations can form crystals early, grows during the thermal decomposition and can lead to non-uniform crystallite size distribution and large particles. In Fig. 5(a) and (b) is possible to see the uniform particle size distribution. The processing temperature is another crucial variable to control the primary particle size. If the temperature is low, the crystallinity of the particles may be affected, yielding poorly crystalline or amorphous particles, as can be seen in Fig. 2, or even incomplete decomposition of organic. However, if the temperature is too high, it enhances the particle growing. In presence of NH_4^+ ions, we expect all the carboxylate groups are dissociated. The polyacrylate/metal ions ratio is also very important to control both agglomerates and primary particles sizes as well as the primary particle crystallinity. Low polyacrylate/metal ratio leads to insufficient carboxylate sites and consequently free metallic ions (as discussed before), and also to low combustion heat, which may affect the crystallinity and reduces the specific surface area [26]. On the other hand, if too much polyacrylate is used, during the thermal decomposition too much CO or CO_2 is generated [26], reducing the partial O_2 pressure, modifying the cation oxidation state and may also generates defects as oxygen vacancies. Another consequence of high ratio is the enhancement of the crystallite size and decrease in the specific surface area [27].

The temperature applied in this study (480 °C) was very similar to that used by other researchers [6,8] for polymeric precursor-based methods [7], even when other oxides were synthesized [18,20]. This method offers the advantage of suppress the aging step, common in polymeric-based synthesis, and yields nanoparticles of 29 nm in very little time, i.e., about 6–7 h, in comparison to others methods. The particles size is very close to hydrothermal method [1], polymeric-like method [7] and organic salt decomposition [8], requiring simple equipment and processed under normal pressure in comparison to other methods [1,10,14,15]. Another advantage is the aqueous-based complexation over non-aqueous-based synthesis [14,15], which occur in few seconds and was dried fast. Compared to the conventional polymeric precursor method, only the aging step is time consuming, since it may exceed 12 h.

The fast and easy technique presented here enabled the synthesis of spinel cobalt oxide nanoparticles in only 6–7 h (note that the complexation step took only 10 min), and precluded the aging step, common in technique based on polymeric precursor as sol–gel and the very long time of the evaporation step required in Pechini method.

4. Conclusions

In summary, this work involved the synthesis of nanoparticles. The modified polymeric precursor method proved efficient, yielding pure and highly crystalline spinel-type cobalt oxide with an average particle size of 29 ± 7 nm measured by TEM. The complexation reaction was inferred to be the chelation type, and, because the cobalt coordination number (4 or 6), it is expected the cobalt ions bind to more than one bonding site (carboxylate) of the same molecule (which for a molecular weight of 4500, each chain has approximately 63 carboxylates), forming a stable structure. The total time required to synthesize the nanoparticles was only 6–7 h, with no aging step and a very rapid complexation step of only 10 min at a relatively low temperature of 480 °C, attesting to the effectiveness, simplicity and speed of this technique.

Acknowledgements

The authors gratefully acknowledge the practical support of the Postgraduate Program in Materials Science and Engineering of the Federal University of São Carlos (PPG-CEM/UFSCar), and the financial support of the Brazilian research funding agencies CNPq (National Council for Scientific and Technological Development, Process 142911/2009-7) and FAPESP (São Paulo Research Foundation, Process 2008/0425-0).

References

[1] M.Y. Nassar, Size-controlled synthesis of $CoCO_3$ and Co_3O_4 nanoparticles by free-surfactant hydrothermal method, Mater. Lett. 94 (2013) 112–115.
[2] J. Gajendiran, V. Rajendran, Preparation of Co_3O_4/carbon nanocomposite and their structural, optical and magnetic studies, Mater. Sci. Semicond. Process. 17 (2014) 59–62.

[3] Y. Li, J. Zhao, Y. Dan, D. Dechong, Y. Zhao, S. Hou, H. Lin, Z. Wang, Low temperature aqueous synthesis of highly dispersed Co_3O_4 nanocubes and their electrocatalytic activity studies, Chem. Eng. J. 166 (2011) 428–434.
[4] J. Xu, J. Cai, J. Wang, L. Zhang, Y. Fan, N. Zhang, H. Zhou, D. Chen, Y. Zhong, H. Fan, H. Shao, J. Zhang, C. Cao, Facile synthesis of hierarchically porous Co_3O_4 nanowire arrays with enhanced electrochemical catalysis, Electrochem. Commun. 25 (2012) 119–123.
[5] X. Lou, J. Han, W. Chu, X. Wang, Q. Cheng, Synthesis and photocatalytic property of Co_3O_4 nanorods, Mater. Sci. Eng., B 137 (2007) 268–271.
[6] W. Li, L. Xu, J. Chen, Co_3O_4 nanomaterials in lithium-ion batteries and gas sensors, Adv. Funct. Mater. 15 (2005) 851–857.
[7] S. Fan, X. Liu, Y. Li, E. Yan, C. Wang, J. Liu, Y. Zhang, Non-aqueous synthesis of crystalline Co_3O_4 nanoparticles for lithium-ion batteries, Mater. Lett. 91 (2013) 291–293.
[8] V. Bartunek, S. Huber, D. Sedmidubský, Z. Sofer, P. Šimek, O. Jankovský, CoO and Co_3O_4 nanoparticles with a tunable particle size, Ceram. Int. 40 (2014) 12591–12595.
[9] R. Tummala, R.K. Guduru, P.S. Mohanty, Nanostructured Co_3O_4 electrodes for supercapacitor applications from plasma spray technique, J. Power Sources 209 (2012) 44–51.
[10] S. Vijayakumar, A.K. Ponnalagi, S. Nagamuthu, G. Muralidharan, Microwave assisted synthesis of Co_3O_4 nanoparticles for high-performance supercapacitors, Electrochim. Acta 106 (2013) 500–505.
[11] R. Parashar, M. Wan, R.R. Yadav, A.C. Pandey, V. Parashar, Surfactant free synthesis of metal oxide (Co and Ni) nanoparticles and applications to heat propagation in nanofluids, Mater. Lett. 440 (2014) 440–443.
[12] J.D. Lee, Concise Inorganic Chemistry, fourth ed., Chapman & Hall, London, 1991.
[13] K.D. Bhatte, B.M. Bhanage, Synthesis of cobalt oxide nanowires using a glycerol thermal route, Mater. Lett. 96 (2013) 60–620.
[14] Q. Yuanchun, Z. Yanbao, W. Zhishen, Preparation of cobalt oxide nanoparticles and cobalt powders by solvothermal process and their characterization, Mater. Chem. Phys. 110 (2008) 457–462.
[15] A.S. Bhatt, D. Krishna, C. Tai, M. Sridhar, Microwave-assisted synthesis and magnetic studies of cobalt oxide nanoparticles, Mater. Chem. Phys. 125 (2011) 347–350.
[16] A.L. Micheli, Synthesis of ceramic powders using an aqueous organic polymer precursor, Ceram. Int. 15 (1998) 131–139.
[17] R. Roma, M. Morcellet, L. Sarraf, Elaboration of cerium oxide from polyacrylate-metal complexes, Mater. Lett. 59 (2005) 889–893.
[18] R.F.K. Gunnewiek, C.F. Mendes, R.H.G.A. Kiminami, Synthesis of Cr_2O_3 nanoparticles via thermal decomposition of polyacrylate/chromium complex, Mater. Lett. 129 (2014) 54–56.
[19] B.D. Cullity, S.R. Stock, Elements of X-ray Diffraction, third ed., Prentice Hall, Upper Saddle River, 1978.
[20] T. Liu, Y. Xu, J. Zhao, Low-temperature synthesis of $BiFeO_3$ via PVA sol–gel route, J. Am. Ceram. Soc. 93 (2010) 3637–3641.
[21] L.F. Silva, L.J.Q. Maia, M.I.B. Bernardi, J.A. Andrés, V.R. Mastelaro, An improved method for preparation of $SrTiO_3$ nanoparticles, Mater. Chem. Phys. 125 (2011) 168–173.
[22] C.G. Almeida, H.M.C. Andrade, A.J.S. Mascarenhas, L.A. Silva, Synthesis of nanosized β-$BiTaO_4$ by the polymeric precursor method, Mater. Lett. 64 (2010) 1088–1090.
[23] T. Tomida, K. Hamaguchi, S. Tunashima, M. Katoh, S. Masuda, Binding properties of a water-soluble chelating polymer with divalent metal ions measured by ultrafiltration. Poly(acrylic acid), Ind. Eng. Chem. Res. 40 (2001) 3557–3562.
[24] Y.-K. Sun, I.-H. Oh, K.Y. Kim, Synthesis of spinel $LiMn_2O_4$ by the sol–gel method for a cathode-active material in lithium secondary batteries, Ind. Eng. Chem. Res. 36 (1997) 4839–4846.
[25] Y.-K. Sun, I.-H. Oh, S.-A. Hong, Synthesis of ultrafine $LiCoO_2$ powders by the sol–gel method, J. Mater. Sci. 31 (1996) 3617–3621.
[26] D.-H. Chen, X.-R. He, Synthesis of nickel ferrite nanoparticles by sol–gel method, Mater. Res. Bull. 36 (2001) 1369–1377.
[27] H. Taguchi, D. Matsuda, M. Nagao, H. Shibahara, Synthesis of $LaMn0_3$ using poly(acrylic acid), J. Mater. Sci. Lett. 12 (1993) 891–893.

Please cite this article in press as: R.F.K. Gunnewiek et al., Synthesis of spinel cobalt oxide nanoparticles using a modified polymeric precursor method, Advanced Powder Technology (2016), http://dx.doi.org/10.1016/j.apt.2016.03.013